

# Detection of long nulls in PSR B1706–16, a pulsar with large timing irregularities.

Arun Naidu,<sup>1,2\*</sup> Bhal Chandra Joshi,<sup>1†</sup> P.K Manoharan<sup>1,3</sup> and M.A Krishnakumar<sup>1,3</sup>

<sup>1</sup>National Centre for Radio Astrophysics, Pune, India

<sup>2</sup>McGill Space Institute, McGill University, Montreal, Quebec, Canada

<sup>3</sup>Radio Astronomy Centre, Udhagamandalam, Tamilnadu, India

Accepted for publication in MNRAS.

## ABSTRACT

Single pulse observations, characterizing in detail, the nulling behaviour of PSR B1706–16 are being reported for the first time in this paper. Our regular long duration monitoring of this pulsar reveals long nulls of 2 to 5 hours with an overall nulling fraction of  $31 \pm 2\%$ . The pulsar shows two distinct phases of emission. It is usually in an active phase, characterized by pulsations interspersed with shorter nulls, with a nulling fraction of about 15 %, but it also rarely switches to an inactive phase, consisting of long nulls. The nulls in this pulsar are concurrent between 326.5 and 610 MHz. Profile mode changes accompanied by changes in fluctuation properties are seen in this pulsar, which switches from mode A before a null to mode B after the null. The distribution of null durations in this pulsar is bimodal. With its occasional long nulls, PSR B1706–16 joins the small group of intermediate nullers, which lie between the classical nullers and the intermittent pulsars. Similar to other intermediate nullers, PSR B1706–16 shows high timing noise, which could be due to its rare long nulls if one assumes that the slowdown rate during such nulls is different from that during the bursts.

**Key words:** pulsars – nulling

## 1 INTRODUCTION

Pulsars are highly magnetized rotating neutron stars, which emit coherent beamed electromagnetic emission at the expense of their rotational energy, effectively slowing down the star. Their pulsed emission varies from pulse to pulse. Absence of this pulsed emission for several pulsar rotations was first noted by [Backer \(1970\)](#) in four pulsars. This phenomenon, called pulse nulling, has since been seen in more than 100 pulsars to date ([Wang et al. 2007](#); [Biggs 1992](#); [Ritchings 1976](#); [Burke-Spolaor et al. 2012](#); [Gajjar et al. 2012, 2014a](#)). The duration of nulls varies not only from one pulsar to other, but also for a given pulsar. The percentage of pulses without detectable emission is called nulling fraction (NF), which ranges from few percent to more than 90 percent. While pulsars such as PSR B0835–41 and B2021+51 show mostly single pulse nulls ([Gajjar et al. 2012](#)), no emission is seen in PSR B0826–34 for 15000 pulses ([Durdin et al. 1979](#)). Previously discovered intermittent pulsars such as PSR B1931+24 ([Kramer et al. 2006](#)), PSR J1841–0500

([Camilo et al. 2012](#)), PSR J1832+0029 ([Lorimer et al. 2012](#)), PSR J1107–5907 ([Young et al. 2014](#)), PSR J1910+0517 and J1929+1357 ([Lyne et al. 2017](#)), where no pulsed emission is observed from few days to several years, can also be considered as neutron stars with an extreme form of nulling. Interestingly, the rate of slowdown ( $\dot{\nu}$ ) is reduced in these intermittent pulsars during their inactive phase suggesting changes in torque ([Kramer et al. 2006](#); [Lyne 2009](#)). Changes in magnetosphere state were proposed to explain the inactive phase in these pulsars as this steers the emission beam away from the line of site in addition to a change in slowdown rate ([Timokhin 2010](#)). Hence, some form of rotation rate irregularities are expected in pulsars, which fall in between classical nullers and intermittent pulsars.

In recent years, there is a growing class of such intermediate nullers with nulling time scales of a few hours. Good examples are PSRs like B0823+26 ([Young et al. 2012](#)), PSR J1717–4054 ([Johnston et al. 1992](#)), PSR J1634–5107 ([O’Brien et al. 2006](#)) and PSR J1853+0505 ([Young et al. 2015](#)). Frequent emission of long nulls results in high NFs (> 70%) for all these pulsars. Unlike the intermittent pulsars, where the change in  $\dot{\nu}$  can be estimated during the absence of emission for several days, it is difficult to estimate

\* E-mail: arun@ncra.tifr.res.in

† E-mail: bcj@ncra.tifr.res.in

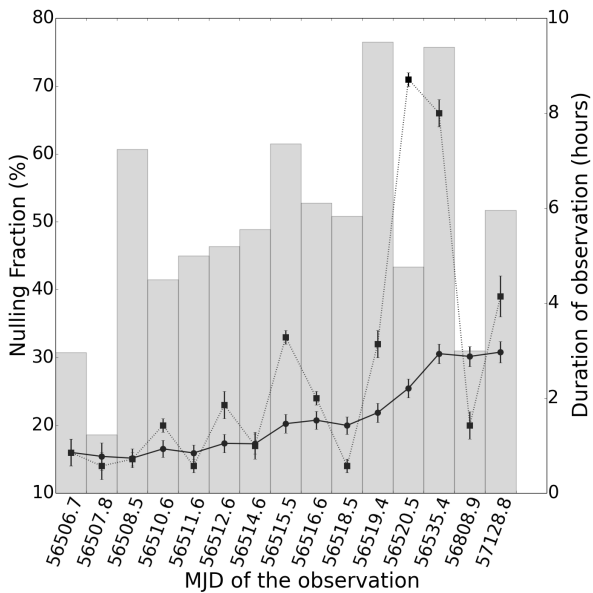


**Figure 1.** Histogram showing the date of observations, duration of observations (bars in the histogram) and corresponding nulling fractions. The dotted line represents the nulling fraction at each epoch and the solid line represents the cumulative nulling fraction with error bars. The ordinate on the left represents the nulling fraction and that on the right represents duration of observations at each epoch.

the slowdown rates for intermediate nullers as the duration of null phase is not long enough to see a significant difference through pulsar timing.

In this paper, detailed single pulse observations of PSR B1706–16 (PSR J1709–1640), discovered in one of the initial Molonglo surveys (Large et al. 1969), are presented. It is like any other normal pulsar with a period of 653 ms and dispersion measure (DM) of  $24.8733 \text{ pc/cm}^3$  (Table 1). While no nulling was reported even 4 decades after its discovery, it was identified as nuller in a single pulse follow up study of High Time Resolution Universe survey (Burke-Spolaor et al. 2012). Its single pulse studies are also relatively undocumented. The pulsar also shows an interesting red noise distribution of the timing residuals as reported by Baykal et al. (1999). In our study, PSR B1706–16 has shown long nulls ( $> 2$  hrs) about once in a week making this a unique addition to the class of intermediate nullers. In Section 2, the observations are described. The description of analysis and results is in Section 3 followed by discussions and conclusions in Section 4 and Section 5 respectively.

## 2 OBSERVATIONS

All the 325 MHz observations were carried out using the Ooty Radio Telescope [ORT, Swarup et al. (1971)], which is a single dish cylindrical parabolic reflector with linearly polarized dipole feed. Data were recorded by using the newly commissioned pulsar receiver PONDER (Naidu et al. 2015). The frequency of observations was 326.5 MHz with a bandwidth of 16 MHz. The ORT has a capability to track PSR

B1706–16 for about 9.5 hours. A total of 15 long duration observations were carried out for this pulsar. The duration of observations varied from 2 hours to 9.5 hours (see Figure 1). All the data were recorded after incoherent dedispersion at the pulsar’s nominal DM of  $24.873 \text{ pc/cm}^3$  and timeseries was provided in SIGPROC<sup>1</sup> format. Further, daily short observations were carried out over a period of four months to check for any timing irregularities and to obtain an updated timing solutions for the analysis.

In addition, simultaneous multi-frequency observations were carried out using the Giant Meterwave Radio Telescope (GMRT) (Swarup et al. 1991) and the ORT for this pulsar. The data at the GMRT were obtained using the GMRT Software Backend (GSB) (Roy et al. 2010) in a phased array mode, where closely spaced 15 antennas were phased to form a single beam in the sky. The GMRT observations were carried out at 610 MHz with a bandwidth of 33 MHz. The data obtained with the GMRT were channelized (512 channels) total intensity data sampled at  $122 \mu\text{s}$ . These data were further analyzed offline using the SIGPROC pulsar analysis software.

## 3 ANALYSIS AND RESULTS

### 3.1 Single pulse sequences and long nulls

The dedispersed data from the ORT observations was folded using the predictors generated with the TEMPO2<sup>2</sup> software to produce the single pulse sequences as shown in the Figure 2. Figure 2(a) shows the typical sequence obtained in 11 of the 15 long observing sessions. The pulsar is usually in an active state with short nulls of null duration not more than 150 periods, which are easy to identify as the single pulses can be seen with high signal to noise ratio (S/N). Figure 2(b), (c) and (d) show 3 out of 4 observing sessions, where long nulls were observed, with each long null lasting between 1 hour to 4.5 hours. This nulling behaviour is rare, with the pulsar exhibiting two different phases, an Active Phase (AP), with pulsed emission seen in most periods, interspersed by short nulls, and an Inactive Phase (IP), where it switches off for few hours with no pulsations at all, similar to other intermediate nulling pulsars (Young et al. 2015). However, unlike the other intermediate nullers, the pulsar is in AP most of the time and rarely switches to the IP.

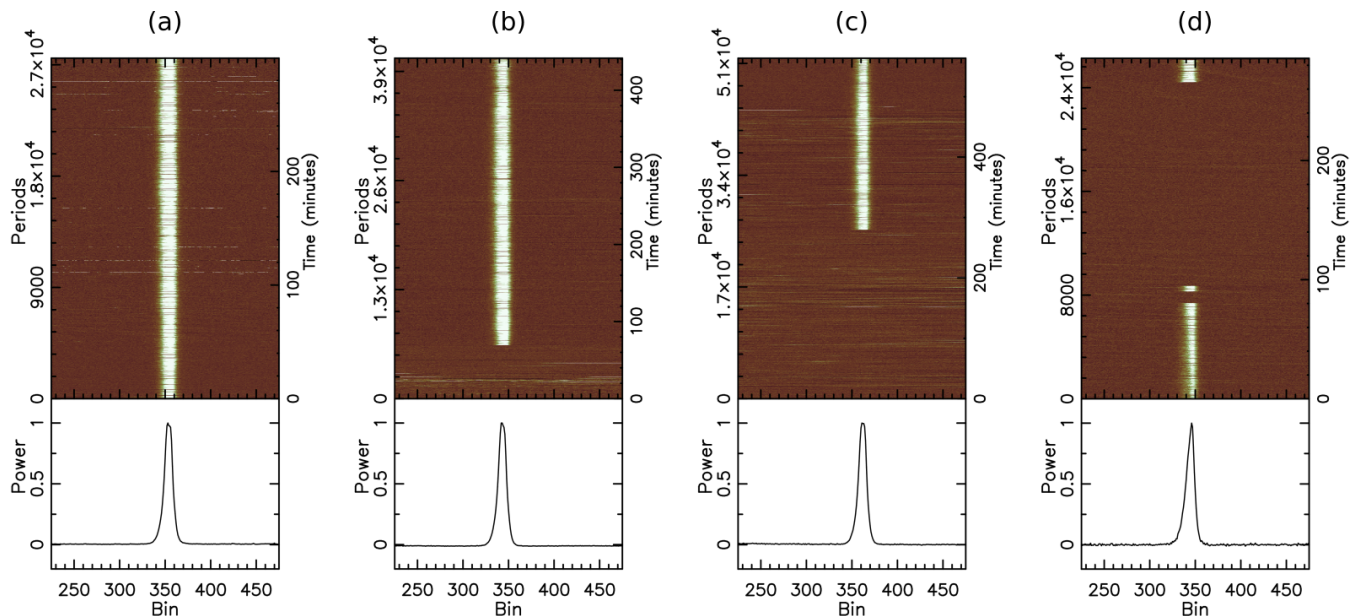
The nulling analysis was performed using the methods devised by Ritchings (1976); Gajjar et al. (2012). These methods, used for estimating the NF and identifying null and burst pulses are briefly described below (For details see Gajjar et al. 2012). We visually identified two windows of equal width in the average profile, namely, a window with phase bins, where the pulsed emission is present (on-pulse window) and another window, away from the pulsed emission (off-pulse window). Two sequences of energies, integrated over on-pulse and off-pulse windows for each pulse, were formed after normalizing with the mean pulse energy. The NF, which represents the percentage of pulses with on-pulse energy distribution similar to that of off-pulse energy, was

<sup>1</sup> <http://sigproc.sourceforge.net>

<sup>2</sup> <http://tempo2.sourceforge.net/>

**Table 1.** The known parameters for PSR B1706–16

JNAME	Right Ascension (h:m:s)	Declination (d:m:s)	Period (s)	DM (pc cm <sup>-3</sup> )	S <sub>400MHz</sub> (mJy)	Surface Magnetic field (10 <sup>12</sup> G)	Characteristic Age (Myr)
J1709–1640	17:09:26.44	-16:40:57.73	0.653054	24.89	47	2.05	1.64


**Figure 2.** Single pulse plots of PSR B1706–16 for four different observations. The top panel in each figure is the single pulse sequence and the bottom panel is the integrated profile. The ordinate on the left-hand axis in each pulse sequence plot denotes the pulse number, whereas the ordinate on the right-hand axis gives time in minutes. Figure (a) shows the typical single pulses observed with out any significant long nulls. Figures (b), (c) and (d) shows the long nulls observed at three different epochs.

estimated from the distributions of on-pulse and off-pulse energies (See Gajjar et al. 2012, for details). A threshold energy separating the zero energy excess in the on-pulse distribution was used to separate null and burst pulses. An overlap in the peak of zero energy excess and the burst energy in the on-pulse distribution can lead to a mis-identification of nulled (burst) pulses.

A total of approximately 100 hours of data were obtained on B1706–16 in 15 separate long observing sessions. The NF was estimated for each observation and is shown in Figure 1. The bars in the plot represent the duration of observations indicated in hours on the right side of the plot. The dotted line represents the variation of the NF for each observation and the solid line represents the cumulative NF calculated for the total duration of the observations.

NF varies from 15 % to 70 % between observations. This variation is mainly due to presence of long nulls in some observations. The four long nulls detected during our observations are listed in the Table 2. The relatively large NF for the other observations is due to the presence of several 5 to 20 minute nulls during the AP, where the NF is estimated to be  $15 \pm 2$  %. The cumulative NF, considering nulls in AP as well as IP from all observations, is calculated to be  $31 \pm 2$  %. It is to be noted that the pulsar rarely switches to the IP, which makes it difficult to get an accurate NF from short

**Table 2.** The four epochs, where long nulls were observed in PSR B1706–16. In three of these epochs, the null was not bounded by burst pulses on both sides. Hence, only a lower limit on the null duration is listed

MJD of observations	Length of null (Rotations)	Duration of null (hours)
56515.5	$\geq 6393$	$\geq 1.16$
56519.4	$\geq 6194$	$\geq 1.12$
56520.5	15825	2.87
56535.5	$\geq 25850$	$\geq 4.68$

observations. Indeed, the nulling fraction was never reported in the previous studies of this pulsar.

### 3.2 Is nulling broadband in PSR B1706–16?

The single pulses in PSR B1706–06 were observed simultaneously with the ORT at 326.5 MHz and the GMRT at 610.0 MHz for a duration of 1 hour (Figure 3). A short stretch of these observations, shown in this plot, clearly shows the burst and null pulses. All the nulls, including those lasting a single period (not seen in the figure), are observed to be simultaneous. Likewise, the transition from the burst emission to null (and vice versa) is also observed to be simultaneous at both the frequencies. Figure 4 shows the on-pulse energy se-

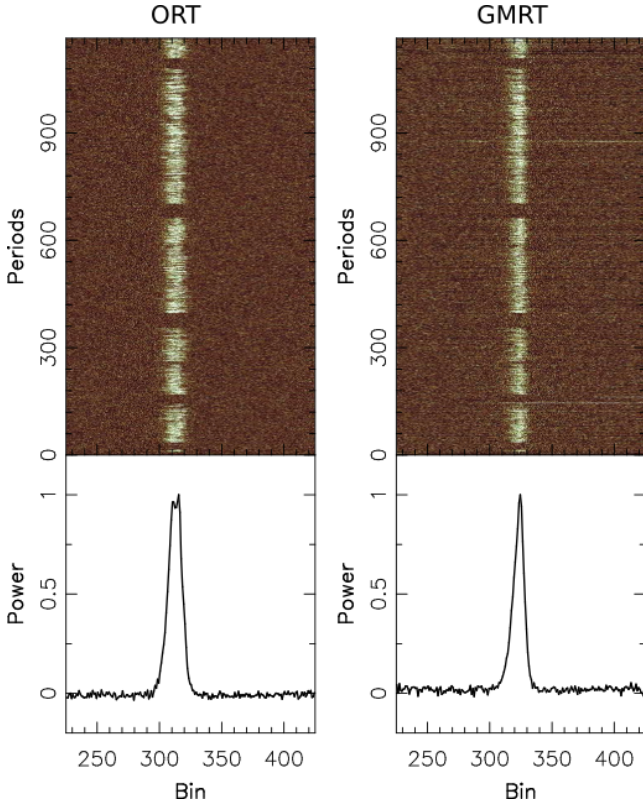


**Figure 3.** Single pulse sequences, observed during the simultaneous observations of PSR B1706–16 using the ORT at 326.5 MHz and the GMRT at 610 MHz

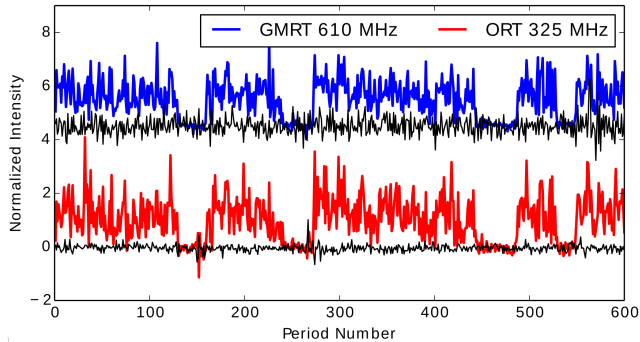


**Figure 4.** Normalized energy in the on-pulse window during 325/610 simultaneous observations shown in the Figure 3. The on-pulse energy at 610 MHz is shown by the blue solid lines, whereas the red lines show the on-pulse energy at 326.5 MHz. The energy integrated over off-pulse window is also shown by solid black line for comparison and identification of nulls.

quence for both the observations for a stretch of 500 periods. The sharp dips in the on-pulse energy in this figure represent the nulls. Again, it is evident that the nulls occur at both frequencies simultaneously. Results from a more quantitative analysis confirming this conclusion are presented below.

Null and burst pulses were identified after a careful visual examination of single pulse sequences at both the frequencies. A one-bit sequence, representing the null and burst

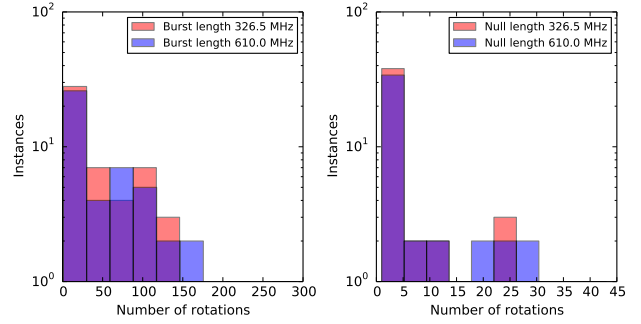


**Figure 5.** Null and burst length histograms of the simultaneous observations.

**Table 3.** Statistics of null and burst pulses in the simultaneous 326.5 and 610 MHz observations of PSR B1706–16.

	Null @ 325 MHz	Burst @ 325 MHz
Null @ 610 MHz	332	2
Burst @ 610 MHz	14	2496

pulses (0 and 1 respectively), was derived from both the observations for 2844 pulses, excluding all the periods affected by radio frequency interference. These one-bit sequences for both the observations of the pulsar were compared using contingency table analysis, where a 2 X 2 table is formed from the two one-bit sequences, giving the statistics of nulls and bursts in the two simultaneous one-bit sequences (Table 3.) In this analysis, the strength of correlation is computed using a  $\phi$ -test and uncertainty tests (Press et al. 1986). The estimated Cramer-V was 0.97 indicating a high significance of correlation, while uncertainty coefficient was estimated to be 0.9, consistent with simultaneity of nulling pattern across frequencies. Moreover, the NF calculated for the ORT and the GMRT observations are  $14 \pm 3$  % and  $12 \pm 1$  % respectively. During the simultaneous observations, no long null was observed. The null and burst length histograms at both the frequencies (Figure 5) were compared using a Kolmogorov-Smirnov test, which rejected, at a high significance ( $\geq 96.9\%$ ), the hypothesis that these two distributions are different. Clearly, nulling is simultaneous at both frequencies, similar to broadband behaviour of nulling demonstrated in a previous studies (Gajjar et al. 2014b; Naidu et al. 2017), increasing the sample of such pulsars.

### 3.3 Average profile of PSR B1706–16

The 610 MHz GMRT observations of PSR B1706–16 show a single component (see Figure 3), which according to the EPN pulsar data base<sup>3</sup> shows a steep linear polarization position angle swing and a circular polarization sense reversal at the center of the component. Thus, this component appears to be a core component (Rankin 1983). The corresponding profile at 326.5 MHz in the simultaneous ORT observations shows two components. This extra component is

<sup>3</sup> <http://www.jb.man.ac.uk/research/pulsar/Resources/epn/>

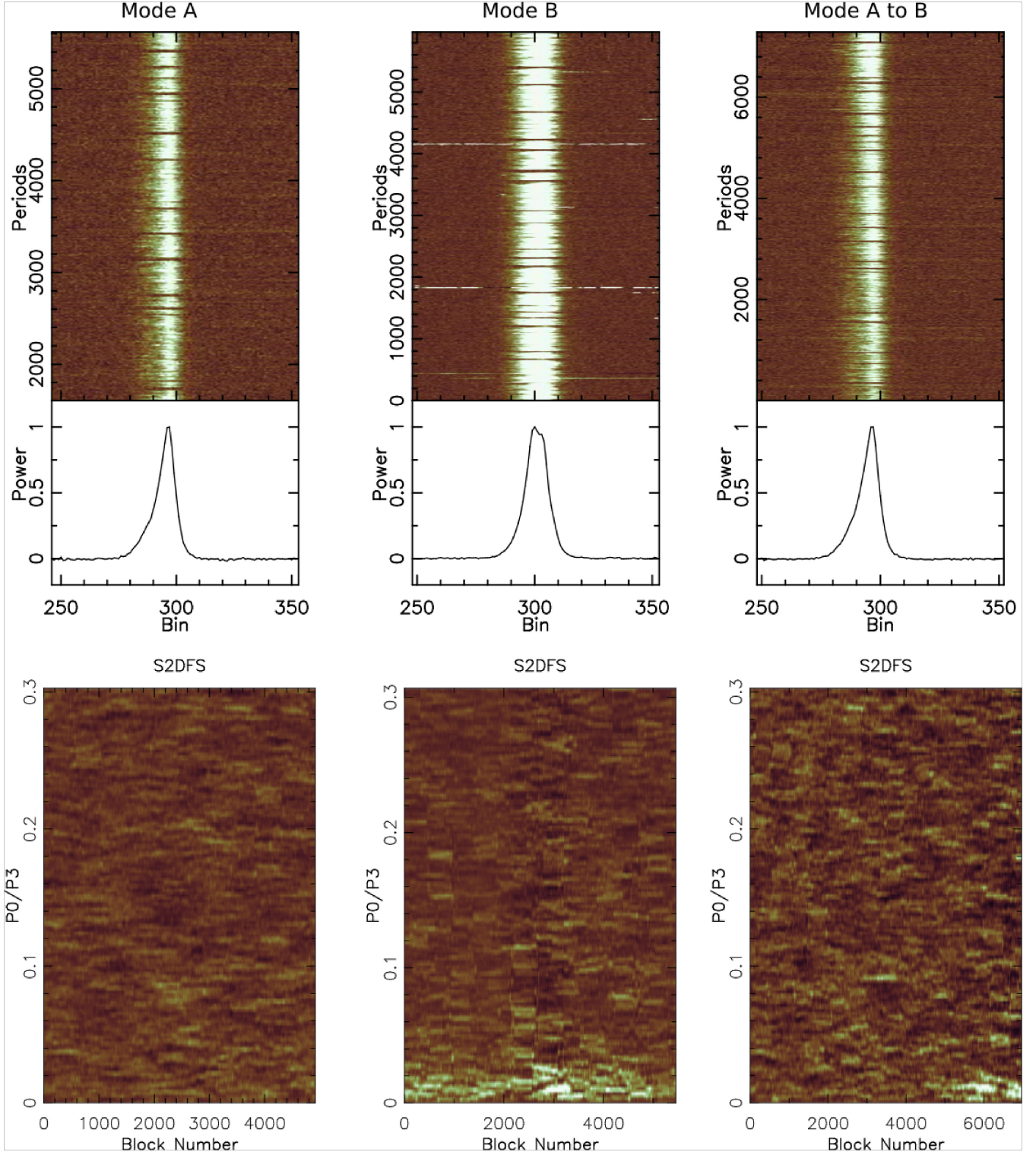


**Figure 6.** Profile modes of PSR B1706–16. Top left plot shows the profile in mode A and corresponding single pulse sequence, which is boxcar averaged with a window size of 20 pulses. The corresponding S2DFS plot is shown in bottom. Top middle plot is profile of mode B with corresponding boxcar averaged pulse sequence and corresponding S2DFS plots at the bottom. The right top plot shows an observed mode change in the pulsar. The pulsar is in mode A in the first 5500 pulses and switches to mode B beyond. This manifests as a drifting signature appearing after 5500 pulses in the corresponding S2DFS plots in the bottom.

**Table 4.** Results of Kolmogorov-Smirnov shape comparison test (Porter 2008) between the profiles shown in Figure 6. A significance close to 1 indicates that the two profiles are similar and vice-versa

No	profiles	Significance
1	mode A and mode B	0.13
2	before null and after null	0.23
3	mode A and before null	0.99
4	mode A and after null	0.34
5	mode B and before null	0.25
6	mode B and after null	0.94

absent from archival profile in EPN pulsar data base, which suggests that we may have observed a profile mode change in our simultaneous ORT observations. The EPN archival profile at 408 MHz shows circular polarization sense reversal towards the trailing dominant component. Hence, it appears that the extra leading component is a conal component. Subpulse drift, manifested as a fluctuation periodicity, is expected in this leading component as this is usually seen in conal components (Rankin 1983). Indeed, we see evidence for this, as discussed in Section 3.4, alongwith changes in average profile.

### 3.4 Profile modes of PSR B1706–16

As mentioned above, this pulsar seems to exhibit two different profile modes at 325 MHz. In mode A, a single component profile is seen, while a two component profile is observed in mode B (Figure 6). One way to check if the two profiles are not similar is to treat them as histograms and perform a Kolmogorov-Smirnov shape comparison test described in Porter (2008). Results are shown in Table 4, which imply that the profiles for the two modes are distinct from each other. The two modes are characterized by distinct fluctuation properties. As can be seen in Figure 6, mode B is accompanied by subpulse drifting, which is associated with the leading component in mode B, while no significant drift feature is detected in mode A (Figure 6). The rightmost plots in Figure 6 shows such Sliding window two dimensional fluctuation spectra (S2DFS, Serylak et al. 2009; Naidu et al. 2017) plot, where this transition from mode A to mode B is clearly visible at about 5500 periods.

It should be noted that the ORT is a single polarization instrument. If a pulsar is highly polarized and has small rotation measure (RM), the profile shape can change due to rotation of polarization angle (PA) with respect to the telescope feed. PSR B1706–16 has a small degree of linear polarization and circular polarization [11 and 6 % (Gould & Lyne 1998)]. It has a small RM of  $-1.3 \text{ rad}/m^2$  (Hamilton & Lyne 1987) resulting in a swing in polarization angle across 16 MHz band of about 6 degrees. Thus, the effect of change in PA cannot produce as significant profile change as seen in Figure 6 as most of the emission is unpolarized. Moreover, it is evident from S2DFS in Figure 6 that the fluctuation properties of profile also change when a profile mode change takes place with variable but clear drifting seen in the mode B. Thus, the profile change between the two modes in PSR B1706–16 is not due to instrumental effects, but is real. The

two profile modes accompanied by changes in drift mode for this pulsar are being reported for the first time in this paper.

### 3.5 Average profile before and after null and during nulls

The visual examination of the emission from PSR B1706–16 before a typical null suggests that the emission seems to diminish gradually (Figure 4). The mean pulse intensity just before the null is less than that for the full data suggesting that the pulsar switches off to the null state gradually. This behaviour appears similar to PSR J1752+2359, where differences in profiles between last pulse before a null and the one after the null were reported by Gajjar et al. (2014a). Hence, we investigated the emission before and after nulls. We selected 10 pulses before and after every null. The left plot in Figure 7 shows the profile just after the null (red) and before the null (green) along with the total average profile (blue) and the null profile (cyan) for all 15 observations. This behaviour is observed in all individual data sets of PSR B1706–16. The pulses just after the null were observed to be of much higher intensity than those observed on an average in this pulsar. Moreover, the before null profile seems to be similar to mode A and profile just after the null is similar to mode B. An analysis using K-S shape comparison test also confirms this conclusion (See Table 4).

Nulls are usually defined as pulses with no detectable emission. However, this does not seem to be strictly true for all nulls in PSR B1706–16. The right plot in the Figure 7 shows the average profiles for nulls with various null duration using all observations. The average null profile for all nulls shows a weak pulse, which is probably due to nulls with duration less than one hour (blue and green). On the other hand, no emission is seen for long nulls ( $> 1$  hour). The ratio of total energy in average profile to null profile is about  $\sim 1420$ . To the best of our knowledge, this is the largest drop in the pulsed emission during the nulls ever reported [see Vivekanand & Joshi (1997); Gajjar et al. (2012, 2014b)].

### 3.6 Distribution of burst and null duration

#### 3.6.1 Burst duration distribution

The distribution of the duration for which the pulsar is in the on state (burst) is shown in Figure 8. This distribution is exponential (black line fit), indicating that the pulsar does not have memory about the burst duration after the previous null. The slight excess of the short bursts may be due to mis-identification of a few short nulls as bursts. As discussed in Section 3.1, such mis-identification results from the overlap between the zero excess and the burst part of on-pulse energy distributions.

#### 3.6.2 Null duration distribution

The distribution of the null duration of the pulsar, shown in the right plot of the Figure 8, is bimodal. Short nulls of few rotations significantly out number the longer nulls extending to tens of rotations. This is partially due to mis-identification of weak low S/N burst pulses as nulls, which could also be the most probable explanation for the weak profile seen after averaging all nulls of duration less than 10 periods (Figure

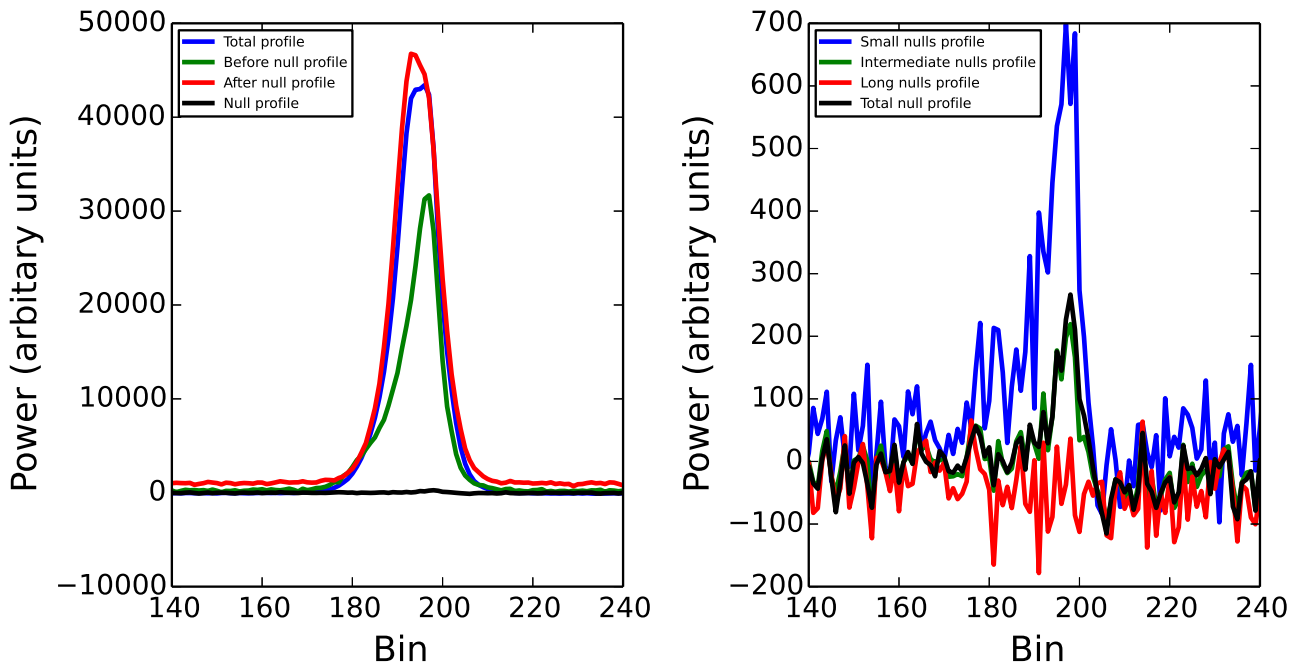


**Figure 7.** Plot on the left shows profiles for 4 different sections of data, 1) Average profile after integrating all the observations (blue), 2) Average profile after integrating 10 pulses just before every null for 15 long observations with about 7500 nulls (green), 3) Average profile after integrating 10 pulses just after every null for the 15 long observations (red), 4) Average profile for all the nulled pulses (black). Plot on right shows average null profiles for nulls with different null duration 1) null profile obtained after averaging all nulls (black). 2) Null profile obtained after averaging all nulls which are less than 10 periods (blue). 3) Null profile obtained after averaging all the intermediate nulls ( $> 10$  periods) shown in green. 4) Null profile obtained after averaging the 4 long nulls in Table 2 (red).

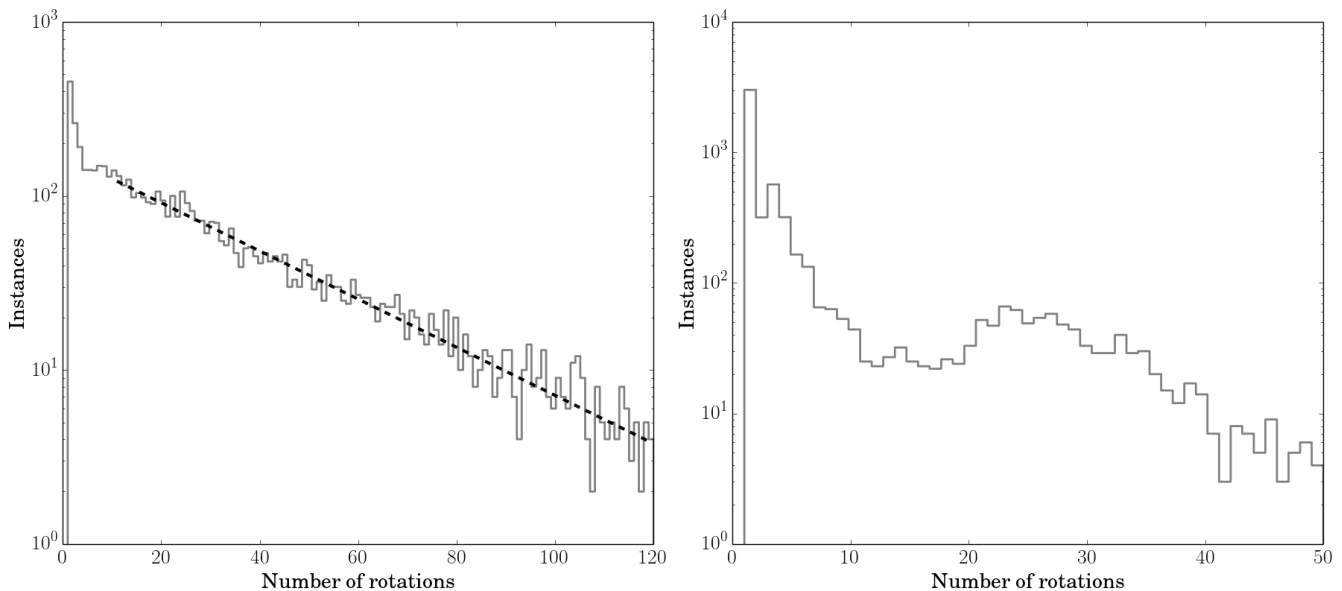


**Figure 8.** Burst length (left plot) and null length (right plot) distributions.

7). However, very few pulses are likely to be mislabeled with most of these being single period nulls. Thus, the bi-modality appears to be genuine. A similar behavior was reported for PSR B0031–07 (Vivekanand 1995)

#### 4 DISCUSSION

Our observations show that PSR B1706–16 has a NF of  $15 \pm 2\%$  during the AP and shows sporadically very long nulls. The longest null duration identified is at least 4.68 hours. Its overall NF is  $31 \pm 2\%$ . Simultaneous two frequency

observations show that nulling in this pulsar is broadband. We have, for the first time, identified two profile modes in this pulsar, which are accompanied by difference in the fluctuation properties of single pulses. While the emission during the long nulls drops by a factor of 1420, weak emission is seen in an average profile of short nulls. We also report for the first time a change in profile before and after nulls, with the profile before the null similar to mode A profile and that after a null similar to mode B. Finally, a bimodal distribution for null length is reported.

This interesting nulling behaviour is reported for the first time for this pulsar. The variability in NF from one observing session to other (Figure 1) implies that NF, at best, provides a qualitative description of nulling and is not an appropriate parameter to look for correlation with other pulsar parameters as was done in some previous studies [e.g. see Biggs (1992)]. Nulling is likely to be better characterized by the nulling pattern or null length distribution, as was also shown by Gajjar et al. (2012). This motivates longer than usual 1 hour observations to determine these distributions before a comparison with pulse period, magnetic field or spin-down energy loss can be done.

The simultaneity of nulling at 326.5 MHz and 610 MHz, seen in PSR B1706–06, is consistent with the previous multi-frequency studies of three pulsars, where the nulling was reported to be broadband (Gajjar et al. 2014b). Broadly, there are two different explanation for pulse nulling. The first class of models invokes intrinsic changes in the magnetospheric physics to explain nulling, whereas the second class invokes geometry as explained in Gajjar et al. (2014b). Our result further strengthens the possibility that intrinsic changes are responsible for nulling rather than the geometrical effects, such as traverses of the line-of-sight through the gaps between the sub beams (pseudo-nulls).

The difference in pulse profile shape with different drift modes has been reported in a couple of previous studies in PSR B0031–07 and B2319+60 (Wright & Fowler 1981; Vivekanand & Joshi 1997; Joshi 2013). Similar behaviour in PSR B1706–06 further strengthens the possibility that the profile mode changes alongwith the nulls are probably related to changes in pulsar magnetosphere.

Most pulsars show exponential or log-normal distributions for their null duration. The notable exceptions are PSR B0031–07 (Vivekanand 1995), J1717–4054 (Kerr et al. 2014), J1649+2533 and B2310+42 (Wright et al. 2012), where bimodal nulling distributions have been reported. PSR B1706–06 also shows a bimodal distribution representing short as well as long nulls. Together with the on-state (or more precisely two different on-states if the two profile modes are taken into account), this represents a multi-state Markov process for such state switching as proposed recently (Gajjar et al. 2012; Cordes 2013), which could arise from a combination of modulation of ion and electron currents within a range of extreme vacuum and force-free state (Li et al. 2012a,b).

The non-white distribution in the timing analysis of the PSR B1706–16 (Baykal et al. 1999; Hobbs et al. 2010) suggests that this pulsar exhibits varying slowdown rates ( $\dot{\nu}$ ) with time. If the pulsar undergoes changes in slowdown rate during the nulls with random null duration, it manifests as timing noise in the residuals for the pulsar. We also see evidence for such timing noise in our data. Such variable  $\dot{\nu}$

was attributed to switching between distinct magnetospheric states for intermittent pulsars (Timokhin 2010). While the intermediate nature of nulls in PSR B1706–16 does not permit establishing this clearly, a higher timing noise is certainly expected in this model.

Classical nullers are known to have off-state ranging upto several minutes in contrast to intermittent pulsars (which null for several days) and Rotating Radio transients (RRATs, which show isolated single period bursts separated by several periods). Long nulls reported by us place PSR B1706–16 in the growing class of intermediate nullers which lie between the classical nullers and intermittent pulsars. The intermediate nullers and intermittent pulsars are a useful way to probe the effect of magnetospheric changes on pulsar timing (Lyne et al. 2010). While the latter require a several years to study their timing behaviour, intermediate nullers provide a tool for such studies in a smaller time-scale.

It is useful to compare and contrast the nulling behaviour of PSR B1706–06 with that of other known intermediate nullers. While the NF for PSR B0823+26 in its AP is estimated to be  $15\pm 1\%$  (Sobey et al. 2015), estimates for other intermediate nullers range from  $67\pm 8\%$  in PSR J1853+0505 to  $90\pm 5\%$  in PSR J1634–5107 (Young et al. 2015). It may be noted that these may be overestimates as the NF were mostly inferred from non-detection/detection statistics in these pulsars. Thus, the NF for PSR B1706–06 is much smaller in contrast with majority of intermediate nuller. Bimodal null distribution was reported for PSR J1717–4054 (Kerr et al. 2014), while it is not well determined for other intermediate nuller. Thus, more detailed observations of other intermediate nuller are needed to check if this property is shared by this class as a whole. PSRs B0823+26, J1634–5107 and PSR J1853+0505 all show weak emission during longer nulls (Young et al. 2015), whereas we do not detect any weak emission in PSR B1706–16 after integrating all long nulls, although weak emission is seen for shorter nulls in AP. It may be noted that no weak emission was detected in the PSR J1717–4054 (Kerr et al. 2014; Young et al. 2015). Lastly, high timing noise or non-white timing residuals have been noted for PSR J1634–5107 and PSR J1717–4054, while such behaviour is not very apparent in PSR J1853+0505 and B0823+26. The constraints on time scales for IP for the latter two pulsars are not very stringent at the moment and short IP time-scale may explain this difference. Longer (8–10 hrs) and more frequent observations (with a cadence of 1–2 days) of an enhanced sample of intermediate nullers is therefore motivated to investigate a correlation between timing noise and long nulls in these pulsars. Future multi-beam telescopes, such as the SKA, MWA and LOFAR, will be very useful in such studies as they will not only provide higher sensitivity for unambiguous classifications of nulls, but also a commensal way of observing with other pulsar programs, such as search and timing, due to availability of multiple beams.

## 5 CONCLUSIONS

This paper presents the results from the nulling analysis of over 100 hours data on the PSR B1706–16 observed using the ORT. This pulsar is observed in 15 long observations with the duration of observations varying from 2 to

7.5 hours. It exhibits long nulls (null duration of  $> 2$  hours) suggesting that it is an intermediate nuller. Typical intermediate nullers have large nulling fractions ( $> 70\%$ ) due to the frequent long nulls. However, long nulls are seen infrequently, typically once in a week, in this pulsar making it a unique addition to the intermediate nullers list. The over all nulling fraction is estimated to be  $31 \pm 2\%$ . It shows a bimodal distribution for null duration. The pulsar's integrated profile is observed to switch from one mode to another with different fluctuation properties in the two modes.

## ACKNOWLEDGMENTS

We thank the staff of the Ooty Radio Telescope and the Giant Meterwave Radio Telescope for making these observations possible. Both these telescopes are operated by National Centre for Radio Astrophysics (TIFR). This work made use of PONDER backend, built with TIFR XII plan grants 12P0714 and 12P0716. We like to thank the anonymous referee for his/her useful comments and suggestions. BCJ, PKM and MAK acknowledge support for this work from DST-SERB grant EMR/2015/000515.

## REFERENCES

- Backer D. C., 1970, *Nature*, **228**, 42
- Baykal A., Ali Alpar M., Boynton P. E., Deeter J. E., 1999, *MNRAS*, **306**, 207
- Biggs J. D., 1992, *ApJ*, **394**, 574
- Burke-Spolaor S., et al., 2012, *MNRAS*, **423**, 1351
- Camilo F., Ransom S. M., Chatterjee S., Johnston S., Demorest P., 2012, *ApJ*, **746**, 63
- Cordes J. M., 2013, *ApJ*, **775**, 47
- Durbin J. M., Large M. I., Little A. G., Manchester R. N., Lyne A. G., Taylor J. H., 1979, *MNRAS*, **186**, 39P
- Gajjar V., Joshi B. C., Kramer M., 2012, *MNRAS*, **424**, 1197
- Gajjar V., Joshi B. C., Wright G., 2014a, *MNRAS*, **439**, 221
- Gajjar V., Joshi B. C., Kramer M., Karuppusamy R., Smits R., 2014b, *ApJ*, **797**, 18
- Gould D. M., Lyne A. G., 1998, *MNRAS*, **301**, 235
- Hamilton P. A., Lyne A. G., 1987, *MNRAS*, **224**, 1073
- Hobbs G., Lyne A. G., Kramer M., 2010, *MNRAS*, **402**, 1027
- Johnston S., Lyne A. G., Manchester R. N., Kniffen D. A., D'Amico N., Lim J., Ashworth M., 1992, *MNRAS*, **255**, 401
- Joshi B. C., 2013, in van Leeuwen J., ed., IAU Symposium Vol. 291, Neutron Stars and Pulsars: Challenges and Opportunities after 80 years. pp 414–416, doi:10.1017/S1743921312024325
- Kerr M., Hobbs G., Shannon R. M., Kiczynski M., Hollow R., Johnston S., 2014, *MNRAS*, **445**, 320
- Kramer M., Lyne A. G., O'Brien J. T., Jordan C. A., Lorimer D. R., 2006, *Science*, **312**, 549
- Large M. I., Vaughan A. E., Wielebinski R., 1969, *Nature*, **223**, 1249
- Li J., Spitkovsky A., Tchekhovskoy A., 2012a, *ApJ*, **746**, 60
- Li J., Spitkovsky A., Tchekhovskoy A., 2012b, *ApJ*, **746**, L24
- Lorimer D. R., Lyne A. G., McLaughlin M. A., Kramer M., Pavlov G. G., Chang C., 2012, *ApJ*, **758**, 141
- Lyne A. G., 2009, in Becker W., ed., Vol. 357, Astrophysics and Space Science Library. p. 67, doi:10.1007/978-3-540-76965-1\$.54
- Lyne A., Hobbs G., Kramer M., Stairs I., Stappers B., 2010, *Science*, **329**, 408
- Lyne A. G., et al., 2017, *ApJ*, **834**, 72
- Naidu A., Joshi B. C., Manoharan P. K., Krishnakumar M. A., 2015, *Experimental Astronomy*, **39**, 319
- Naidu A., Joshi B. C., Manoharan P. K., Krishnakumar M. A., 2017, preprint, (arXiv:1704.05048)
- O'Brien J. T., Kramer M., Lyne A. G., Lorimer D. R., Jordan C. A., 2006, Chinese Journal of Astronomy and Astrophysics Supplement, **6**, 4
- Porter F. C., 2008, preprint, (arXiv:0804.0380)
- Press W. H., Flannery B. P., Teukolsky S. A., 1986, Numerical recipes. The art of scientific computing
- Rankin J. M., 1983, *ApJ*, **274**, 333
- Ritchings R. T., 1976, *MNRAS*, **176**, 249
- Roy J., Gupta Y., Pen U.-L., Peterson J. B., Kudale S., Kodilkar J., 2010, *Experimental Astronomy*, **28**, 25
- Serylak M., Stappers B. W., Weltevrede P., 2009, *A&A*, **506**, 865
- Sobey C., et al., 2015, *MNRAS*, **451**, 2493
- Swarup G., et al., 1971, *Nature Physical Science*, **230**, 185
- Swarup G., Ananthakrishnan S., Kapahi V. K., Rao A. P., Subrahmanya C. R., Kulkarni V. K., 1991, Current Science, Vol. 60, NO.2/JAN25, P. 95, 1991, **60**, 95
- Timokhin A. N., 2010, *MNRAS*, **408**, L41
- Vivekanand M., 1995, *MNRAS*, **274**, 785
- Vivekanand M., Joshi B. C., 1997, *ApJ*, **477**, 431
- Wang N., Manchester R. N., Johnston S., 2007, *MNRAS*, **377**, 1383
- Wright G. A. E., Fowler L. A., 1981, *A&A*, **101**, 356
- Wright G., Weltevrede P., Rankin J., Herfindal J., 2012, in Lewandowski W., Maron O., Kijak J., eds, Astronomical Society of the Pacific Conference Series Vol. 466, Electromagnetic Radiation from Pulsars and Magnetars. p. 87
- Young N. J., Stappers B. W., Weltevrede P., Lyne A. G., Kramer M., 2012, *MNRAS*, **427**, 114
- Young N. J., Weltevrede P., Stappers B. W., Lyne A. G., Kramer M., 2014, *MNRAS*, **442**, 2519
- Young N. J., Weltevrede P., Stappers B. W., Lyne A. G., Kramer M., 2015, *MNRAS*, **449**, 1495

This paper has been typeset from a  $\text{\TeX}/\text{\LaTeX}$  file prepared by the author.